

## Strain relief guided novel growth of atomic nanowires in a Cu<sub>3</sub>N-Cu(110) molecular network

X. D. Ma, D. I. Bazhanov, Olivier Fruchart, F. Yildiz, T. Yokoyama, M. Przybylski, V. S. Stepanyuk, W. Hergert, J. Kirschner

► **To cite this version:**

X. D. Ma, D. I. Bazhanov, Olivier Fruchart, F. Yildiz, T. Yokoyama, et al.. Strain relief guided novel growth of atomic nanowires in a Cu<sub>3</sub>N-Cu(110) molecular network. Physical Review Letters, American Physical Society, 2009, 102, pp.205503. <10.1103/PhysRevLett.102.205503>. <hal-00378769>

**HAL Id: hal-00378769**

**<https://hal.archives-ouvertes.fr/hal-00378769>**

Submitted on 27 Apr 2009

**HAL** is a multi-disciplinary open access archive for the deposit and dissemination of scientific research documents, whether they are published or not. The documents may come from teaching and research institutions in France or abroad, or from public or private research centers.

L'archive ouverte pluridisciplinaire **HAL**, est destinée au dépôt et à la diffusion de documents scientifiques de niveau recherche, publiés ou non, émanant des établissements d'enseignement et de recherche français ou étrangers, des laboratoires publics ou privés.

# Strain relief guided novel growth of atomic nanowires in Cu<sub>3</sub>N-Cu(110) molecular network

X.-D. Ma,<sup>1</sup> D. I. Bazhanov,<sup>1,2</sup> O. Fruchart,<sup>1,3</sup> F. Yildiz,<sup>1</sup> T. Yokoyama,<sup>4</sup>  
M. Przybylski,<sup>1,\*</sup> V. S. Stepanyuk,<sup>1,†</sup> W. Hergert,<sup>5</sup> and J. Kirschner<sup>1</sup>

<sup>1</sup>*Max-Planck-Institut für Mikrostrukturphysik, Weinberg 2, D-06120 Halle, Germany*

<sup>2</sup>*Moscow State University, GSP-1, Lenin Hills, 119991 Moscow, Russia*

<sup>3</sup>*Institute Nèel (CNRS), BP166, F-38042 Grenoble Cedex 9, France*

<sup>4</sup>*Institute for Molecular Science, Myodaiji-cho, Okazaki, Aichi 444-8585, Japan*

<sup>5</sup>*Martin-Luther-Universität Halle-Wittenberg, Friedemann-Bach-Platz 6, D-06099 Halle, Germany*

(Dated: April 6, 2009)

A self-corrugated Cu<sub>3</sub>N-Cu(110) molecular network shows potential to overcome the element dependence barrier as demonstrated by epitaxial growth of atomic nanowires ( $\sim 1$  nm in width) among various *3d*, *4d*, and *5d* elements. Scanning tunnelling microscopy (STM) shows that all of the investigated atomic nanowires share an identical structure, featuring uniform width, height, orientation and same minimum separation distance. *Ab initio* study reveals that the formation mechanism of atomic nanowires can be directly attributed to a strain relief guided asymmetric occupation of atoms on the originally symmetric crest zone of the corrugated network.

Atomic nanowires are likely to play a vital role in future electronic devices built up at the nanometer scale [1]. As a cost effective method to prepare nanowires on an atomic scale, self-organization methods have drawn a lot of attention. Various self-organizing methods have been reported to prepare atomic nanowires. For instance, atomic chains prepared on metallic vicinal surfaces [2–4], linear arrays of nanostructures on vicinal Si surfaces [5], and many others.

A general phenomenon which has often been observed in self-organizing processes is the dependence of growth behavior on the combination of substrate and element. For example, on vicinal Pt(111), Co tends to form one dimensional atomic chains, while Ni does not due to substantial Pt-Ni intermixing [3]. On vicinal Cu(111) surfaces, Fe forms monoatomic chains while Co gives rise to nanoislands [4]. On flat Ge and Si(001) surfaces, it has been reported that *5d* elements tend to form atomic chains while *4d* elements do not [6]. Although the reason is still under debate, a plausible picture is that the strong relativistic character of the *5d* electronic states leads to the formation of atomic nanowires [7].

In this letter we report on growth behavior of epitaxial atomic nanowires among a variety of *3d*, *4d*, and *5d* elements on a corrugated molecular Cu<sub>3</sub>N network on Cu(110) surface. *Ab initio* calculations are employed to understand the formation principle of the atomic nanowires on Cu<sub>3</sub>N network. In particular, the strain relief guided occupation of atoms is discussed. Moreover, we have confirmed that the Cu<sub>3</sub>N on a Cu(110) surface forms a polar covalently bonded molecular network with band gap exceeding 3 eV, which is similar to the copper nitride on Cu(001) surface [8].

The copper nitride Cu<sub>3</sub>N network was prepared on a clean single crystalline Cu(110) surface [9–12]. N<sub>2</sub> was backfilled into the chamber at  $1 \times 10^{-7}$  mbar and activated by using an ion gun with a beam energy of 0.6 keV.

The N<sup>+</sup> dosing density was kept at  $2.4 \times 10^{12}$  ions/cm<sup>2</sup>s. The N<sup>+</sup> nitriding was performed at a temperature of around 700 K resulting in a fully reconstructed Cu<sub>3</sub>N network with a terrace width of several hundred nanometers and completely free from N<sup>+</sup> sputtering damage. Based on the N<sup>+</sup> dosing density and the dosing duration, the coverage of N was calculated to be around 0.65 ML (1 ML =  $1.1 \times 10^{15}$  atoms/cm<sup>2</sup>, which relates to the density of atoms on the Cu(110) surface).

Fig.1a shows a high-resolution STM image of the Cu<sub>3</sub>N network: the distance between the two nearest bright features along [001] direction is 11 Å and the distance between the two maximally bright features in each chain along [1-10] direction is 5 Å. This structure demonstrates the Cu<sub>3</sub>N network possessing p(2x3) periodicity, which is consistent with the low energy electron diffraction (LEED) pattern (not shown). The Cu<sub>3</sub>N network has corrugation with  $\sim 0.5$  Å depth as shown in the line profile along xx' in Fig.1a. *Ab initio* calculations were carried out to examine the structural details concerning the corrugation of the Cu<sub>3</sub>N network. We used molecular dynamics calculations based on density functional theory as it is implemented in the Vienna *ab initio* simulation package (VASP) [13]. VASP code was used to solve Kohn-Sham equations with periodic boundary conditions and a plane-wave basis set. For total energy and force calculations, we employed an all-electron projector augmented wave (PAW) method [14]. The electron exchange and correlation effects have been taken into account using generalized gradient approximation (GGA) [15]. We used a maximal kinetic energy cut-off of 400 eV which can converge iteratively on the total energy of considered systems to within 1 meV/atom. The integration over Brillouin zone has been performed using the well converged k-meshes of 4x4x1, 4x6x1 and 4x8x1 grids. Structural relaxations were determined via a quasi-Newton algorithm using the exact Hellmann-Feynman forces acting on each

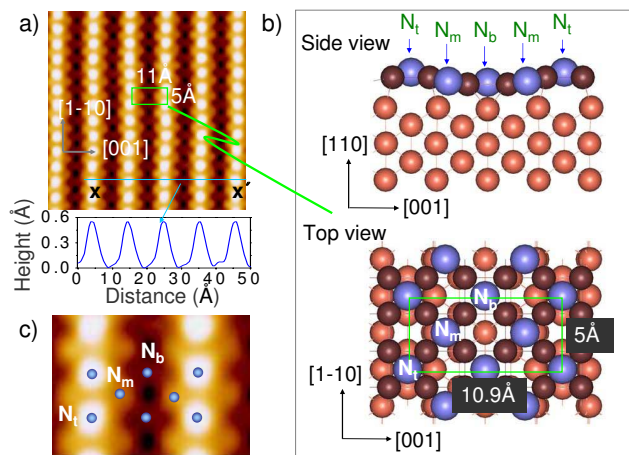


FIG. 1: a, High resolution room temperature STM image ( $60 \text{ \AA} \times 60 \text{ \AA}$ ,  $0.37 \text{ nA}$ ,  $750 \text{ mV}$ ) with line profile along  $xx'$ . b, Schematic view of the atomic structure for one corrugation unit on the  $\text{Cu}_3\text{N}$  network from *ab initio* calculations.  $N_t$ ,  $N_m$ , and  $N_b$  represent the top, middle, and bottom positions, respectively, for N atoms. c, STM image ( $14 \text{ \AA} \times 20 \text{ \AA}$ ) magnified from image a, superimposed upon N atoms based on the structural model. Blue, dark brown, and light brown spheres denote N atoms including  $N_t$ ,  $N_m$ , and  $N_b$  in the top layer of the  $\text{Cu}_3\text{N}$ , Cu atoms in the top layer of the  $\text{Cu}_3\text{N}$ , and Cu atoms below  $\text{Cu}_3\text{N}$  network, respectively.

atom. The Monkhorst-Pack scheme [16] was used for k-point sampling of the Brillouin zone.

We explored two of surface reconstruction models, which have been favored as the most reliable ones according to recent experimental structural studies: the so-called [110]-missing-row model [11] and the pseudo-(100) model [17]. The former model reproduces  $p(2 \times 3)$  surface nitride phase by removing each third row of Cu atoms along the [110] direction. We found that for nitrogen atoms, the subsurface so called long bridge (LB) sites of a substrate are not favorable positions for bonding. They exhibit a strong upward relaxation and prefer to segregate towards the surface, infringing on a 0.66 ML nitrogen coverage requirement.

The pseudo-(100) model involves a formation of a surface nitride  $\text{Cu}_3\text{N}$  within the reconstructed surface layer of Cu(110) substrate, consisting of a nearly square array of Cu atoms with a  $c(2 \times 2)$  arrangement of N atoms (see Fig.1b, top view). This surface nitride structure is similar to that observed for N chemisorption on Cu(001), where nitrogen atoms are adsorbed at the fourfold hollow sites, being nearly coplanar to the reconstructed surface layer [18]. We carried out first-principles calculations to study in detail the structural parameters of the surface nitride phase based on the proposed pseudo-(100) reconstruction model. The obtained results demonstrate that  $p(2 \times 3)$   $\text{Cu}_3\text{N}$  nitride surface phase, represented by a pseudo-(100) surface reconstruction model, exhibits a large expansion of interlayer spacing (about +53%) between surface reconstructed and subsurface unreconstructed cop-

per layers. The corrugation amplitude of  $\text{Cu}_3\text{N}$  network along the [001] direction is about  $0.5 \text{ \AA}$ , which is consistent with the value measured by STM. As shown in Fig.1b, the corrugation of the surface layer results in two raised and two lowered rows of copper atoms with a strong displacement from their original position on the clean Cu(110) surface. Nitrogen atoms form a regular  $c(2 \times 2)$  atomic structure by their adsorption at three different hollow sites (designated as  $N_t$ ,  $N_m$ , and  $N_b$ , - on the top, middle and at the bottom, respectively) within a one trough distance of the corrugated surface copper nitride layer (see Fig.1c). Our calculations indicate Cu and N atoms within the  $\text{Cu}_3\text{N}$  layer are covalently polar bonded yielding a similar molecular network as reported on Cu(100) [8]. The pseudo-(100) surface is rigorously verified by the atomic resolution STM image shown in Fig.1c, where the positions of  $N_t$ ,  $N_m$  and  $N_b$  atoms are superimposed onto the corresponding *ab initio* model. The middle N atoms ( $N_m$ ) are better resolved at the place where the top N atoms, i.e.,  $N_t$  are missed.

Such a  $\text{Cu}_3\text{N}$  network allows a growth of atomic nanowires. All of the nanowires shown in Fig.2a-d were deposited on the  $\text{Cu}_3\text{N}$  network at room temperature (RT) by molecular beam epitaxy (MBE). Nanowires made of different elements show an identical structure. We give a detailed description by taking Fe atomic nanowire as a representative example. Fig.2a shows 0.05 ML of Fe on a  $\text{Cu}_3\text{N}$  network prepared by MBE at a growth rate of  $0.2 \text{ ML/min}$ . The line profile of a single Fe nanowire in Fig.2a shows that the height of the wire is  $\sim 1.23 \text{ \AA}$ . The width at FWHM of the wire is found to be  $11 \text{ \AA}$ , which is verified later by atomic resolution STM of the nanowire, see Fig.3c. As shown in Fig.1b, the calculated width of one trough of the corrugated  $\text{Cu}_3\text{N}$  network is  $10.9 \text{ \AA}$ . This indicates that each individual atomic nanowire occupies a single trough of the  $\text{Cu}_3\text{N}$  network. No width distribution is found for the grown atomic nanowires. An identical structure of atomic nanowires made of different elements on the  $\text{Cu}_3\text{N}$  network is confirmed in Fig.2b-d where atomic nanowires with coverage of 0.2 ML Fe, 0.2 ML Pd and 0.2 ML Au are presented. It is also seen that the Fe nanowires at the coverage of 0.05 and 0.2 ML of Fe are identical. The same nanowire structures for other elements such as Mn, Ni, Rh, Cr, Co are not shown here due to space limit.

A combined high-resolution STM study and *ab initio* calculations were performed to clarify the atomic structure of individual atomic nanowires on the  $\text{Cu}_3\text{N}$ -Cu(110). Based on the surface nitride  $p(2 \times 3)$  structure of the  $\text{Cu}_3\text{N}$  network, we studied the binding properties of the most coordinated adsorption sites with regard to the  $\text{Cu}_3\text{N}$  surface plane. Owing to the corrugation of the  $p(2 \times 3)$   $\text{Cu}_3\text{N}$  nitride phase there are three different fourfold hollow sites (designated in Fig.3a as 1, 3, and 5, for top, intermediate and bottom Fe atoms, respectively), and two different threefold bridge sites (designated as

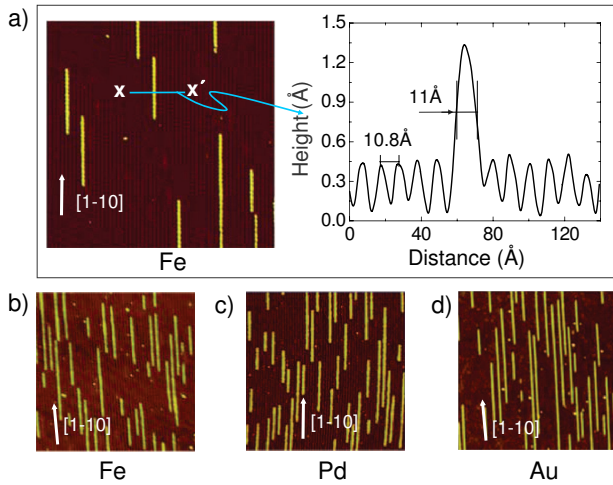


FIG. 2: a, STM image ( $570 \text{ \AA} \times 570 \text{ \AA}$ ,  $0.45 \text{ nA}$ ,  $860 \text{ mV}$ ) of atomic nanowires after deposition of  $0.05 \text{ ML}$  Fe and the line profile along  $xx$ . b, c and d show STM images of atomic nanowires after deposition of  $0.2 \text{ ML}$  of Fe, Pd and Au, respectively (all three STM images are sized  $700 \text{ \AA} \times 700 \text{ \AA}$ ).

2 and 4 for top and bottom Fe atoms) for adsorption within the  $p(2 \times 3)$  unit cell. To simulate Fe nanowires we used a supercell approach. The supercell structure consists of a 6 atomic layer slab of Cu(110) substrate with  $N$  atoms embedded into the upper surface layer and Fe atoms deposited on top of the  $\text{Cu}_3\text{N}$  surface network. The vacuum region between repeated slabs is  $10 \text{ \AA}$ . For all calculations, the two bottom layers of the slab have a fixed interlayer distance of  $1.28 \text{ \AA}$  (which refers to the distance between the nearest crystalline planes along  $[110]$  direction for bulk Cu), while other atomic layers are relaxed until the forces are converged in the supercell. The calculations for adsorbed Fe adatoms on  $p(2 \times 3)$   $\text{Cu}_3\text{N}$  indicate that the bridge sites (2 and 4) are energetically less favorable than the hollow sites (1, 3, and 5). We observe that adsorption of a Fe adatom at the bridge site causes a substantial vertical displacement of the Cu atom directly below this adatom. This Cu atom exhibits a strong relaxation towards the Cu bulk and will no longer be a part of the surface nitride phase. Fe adatoms have a high adhesion at the hollow sites surrounded by copper atoms of  $\text{Cu}_3\text{N}$  network, where the most favorable binding site is at the bottom of the trough (site 5) and the sites 1 and 3 with an energy loss of about  $1.36 \text{ eV}$  and  $1.85 \text{ eV}$  with respect to the site 5, respectively.

We next studied the formation process and structural parameters of the Fe atomic wires on the  $\text{Cu}_3\text{N}$  network. Based on structural information obtained by STM, we examined each Fe atomic wire consisting of individual atomic rows running along the  $[1-10]$  direction and occupying a relatively stable hollow site, one belonging to a single trough of the corrugated  $\text{Cu}_3\text{N}$  network (see Fig.3b). In addition, from Fig.3b one can see that each nanowire consists of five atomic rows with Fe atoms at the top (1), intermediate (3), and bottom (5) adsorption

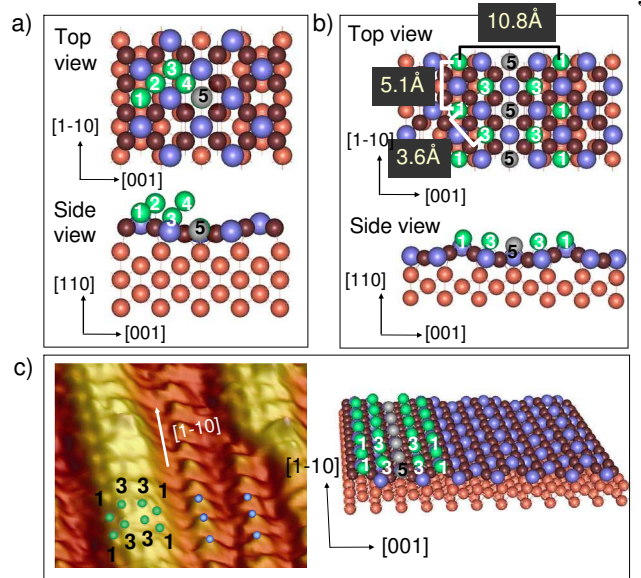


FIG. 3: a, The top view shows three different fourfold hollow sites of the  $\text{Cu}_3\text{N}$  network which are designated as 1, 3, and 5, for the top, intermediate, and bottom Fe atoms, respectively, and two different threefold bridge sites 2 and 4, for top and bottom Fe atoms. The side view shows that the positions of the Fe adatoms at sites 2 and 4, according to the results of *ab initio* calculation, are higher than the ones at other sites. b, Schematic view of the atomic structure of a single Fe nanowire from *ab initio* calculations. Each nanowire is five atomic rows in width. Fe atoms at the top (1), intermediate (3) and bottom (5) adsorption sites are shown in side view. c, STM image of Fe atomic nanowire ( $39 \text{ \AA} \times 48 \text{ \AA}$ ,  $0.46 \text{ nA}$ ,  $500 \text{ mV}$ ) superimposed upon the Fe atom positions from *ab initio* study. The structural model is placed to the right for better understanding. In a, b, and c, blue, dark brown, light brown and light green colors denote all N atoms in the top layer of the  $\text{Cu}_3\text{N}$ , Cu atoms in the top layer of the  $\text{Cu}_3\text{N}$ , Cu atoms below  $\text{Cu}_3\text{N}$  network, and Fe atoms, respectively. Note: The bottom Fe atoms (5) are shown in gray color since they are deeply embedded into  $\text{Cu}_3\text{N}$  network and hence hardly visible in the STM image.

sites of the trough. The nanowires have a width of  $10.8 \text{ \AA}$ , slightly less than the width of a trough ( $10.9 \text{ \AA}$ ), due to attractive interatomic interaction between Fe atoms trying to enhance their bonding at the surface. The theoretical value of this width coincides remarkably well with the experimental value ( $11.0 \text{ \AA}$ ) measured with STM. It is seen in Fig.3b that the Fe atoms are arranged in individual rows, in a zigzag order within the nanowire, with an average bond length of  $3.6 \text{ \AA}$  in inter-row spacing and with a bond length of  $5.1 \text{ \AA}$  along the rows. The obtained spacing is consistent with the geometry of the fcc(110) surface observed on the  $\text{Cu}_3\text{N}$  network. The agreement between theory and experiment is further confirmed by the positions of Fe atoms shown in Fig.3c, where a model of single atomic wire from *ab initio* study and an atomically resolved STM image are presented. It should be noted here that the relaxation of Fe row (5) adsorbed in the bottom of the trough results in the least height

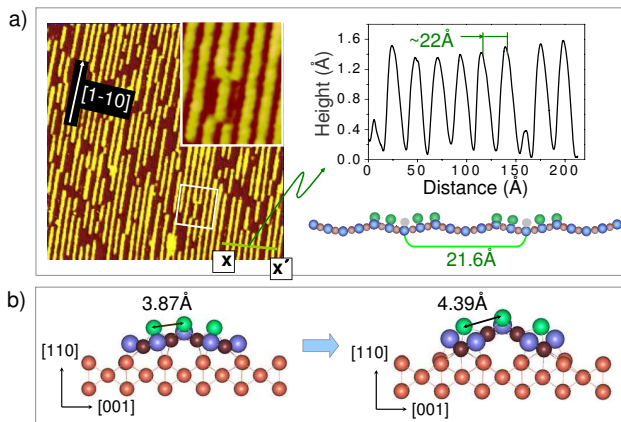


FIG. 4: a, STM image ( $700 \text{ \AA} \times 700 \text{ \AA}$ ,  $0.5 \text{ nA}$ ,  $860 \text{ mV}$ ) of Fe atomic nanowires at coverage of  $0.4 \text{ ML}$  with line profile (right side) along  $xx'$ . The inset magnified image clearly shows that the occupation at the trough nearest to the atomic nanowire is strictly forbidden. The structural model below the line profile is shown to demonstrate the existence of a minimum separation distance. b, The left and right figures show the structure obtained from *ab initio* studies before and after relaxation. Atoms on the crest region become unstable due to the increased Fe-Fe bond distance once both sides of the crest are symmetrically occupied. Here, colors of the atoms are exactly the same as in Fig.3.

( $1.42 \text{ \AA}$ ) above the nearest copper atoms of the surface nitride layer with respect to the other Fe rows. This result explains the absence of bright spots ascribed to the bottom Fe atoms (5) in the middle of the Fe wire, seemingly resulting in the four atomic rows observed by STM, as it is shown in Fig.3c.

As shown in Fig.4a, from the line profile and the structural model below it we found a minimum distance of  $21.6 \text{ \AA}$  between the nanowires, which corresponds exactly to the double periodicity ( $\times 6$ ) of the  $\text{Cu}_3\text{N}$  ( $2 \times 3$ ) network along the  $[001]$  direction. This double periodicity can also be seen in the inset magnified image in Fig.4a, which clearly shows that occupation of the trough nearest to the atomic nanowire is strictly forbidden. This means that a symmetrical occupation on both sides of the crest region between two nearest troughs may be thermodynamically and kinetically unfavorable. We performed calculations for Fe rows deposited on the crest region of a  $p(2 \times 3)$   $\text{Cu}_3\text{N}$  network (one row on top and another two ones at intermediate positions) in order to examine the bonding properties at these positions (see Fig.4b, left). The calculated results show that N atoms in the crest region shift into deposited Fe rows due to their strong covalent bonding with Fe atoms. Formation of Fe-N bonds leads to a large tensile strain propagating across the whole crest region and significantly increasing the inter-row spacing of Fe atoms, up to  $4.39 \text{ \AA}$ , as shown in Fig.4b (right). Thus, the bonding between the Fe rows becomes weak due to bonding competition between Fe-Fe bonds and Fe-N bonds which makes the symmetric occu-

pation on both sides of the crest region thermodynamically unstable. As a consequence, the occupation of Fe atoms becomes asymmetric and only one side of the crest region can be occupied due to the strain relief. Moreover, *ab initio* study has confirmed an observation that within a single trough, five atomic rows of adsorption always lead to the lowest total energy of the system among all of the nanowires with fewer rows. The asymmetric occupation originated from the intrinsic corrugation nature of  $\text{Cu}_3\text{N}$  network indicates that this formation principle can be valid for the other elements, pointing towards the existence of a universal growth behavior on the  $\text{Cu}_3\text{N}$  network.

In summary, we have observed an identical growth behavior of epitaxial atomic nanowires made of different elements on a self-corrugated molecular  $\text{Cu}_3\text{N}$  network prepared on a single crystalline  $\text{Cu}(110)$  surface. All of the atomic nanowires possess an identical structure characterized by uniform width, height and orientation, as well as exhibiting a minimum separation distance corresponding to double periodicity of  $\text{Cu}_3\text{N}$  network along the  $[001]$  direction. *Ab initio* calculations reveal that the common formation principle for these atomic nanowires can be attributed to the strain relief guided asymmetric occupation of atoms at the crest region of  $\text{Cu}_3\text{N}$  network.

We thank H. Menge and G. Kroder for technical support. V. S. S. and W. H. acknowledge financial support from SPP-1165 project.

\* Electronic address: [mprzybyl@mpi-halle.mpg.de](mailto:mprzybyl@mpi-halle.mpg.de)

† Electronic address: [stepanyu@mpi-halle.mpg.de](mailto:stepanyu@mpi-halle.mpg.de)

- [1] W. Yue, J. Xiang, C. Yang, W. Lu, C. M. Lieber, *Nature* **430**, 61 (2004).
- [2] S. Shiraki, H. Fujisawa, M. Nantoh, M. Kawai, *Appl. Surf. Sci.* **237**, 284-290 (2004).
- [3] P. Gambardella, K. Kern, *Surf. Sci.* **475**, L229-L234 (2001).
- [4] J. D. Guo, Y. Mo, E. Kaxiras, Z. Zhang, H. H. Weitering, *Phys. Rev. B* **73**, 193405 (2006).
- [5] T. Sekiguchi, S. Yoshida, K. Itoh, K., *Phys. Rev. Lett.* **95**, 106101 (2005).
- [6] J. Wang, M. Li, E. I. Altman, *Phys. Rev. B* **70**, 233312 (2004).
- [7] A. A. Stekolnikov, F. Bechstedt, M. Wisniewski, J. Schfer, R. Claessen, *Phys. Rev. Lett.* **100**, 196101 (2008).
- [8] F. C. Hirjibehdin, *Science* **317**, 1199 (2007).
- [9] D. Heskett, A. Baddorf, E. W. Plummer, *Surf. Sci.* **195**, 94 (1988).
- [10] A. P. Baddorf, *Phys. Rev. B* **48**, 9013 (1993) and references therein.
- [11] F. M. Leibsle, R. Davis, A. W. Robinson, *Phys. Rev. B* **49**, 8290 (1994).
- [12] S. M. York, F. M. Leibsle, *Phys. Rev. B* **64**, 033411 (2001).
- [13] G. Kresse, J. Hafner, *Phys. Rev. B* **48**, 13115 (1993).
- [14] G. Kresse, J. Furthmuller, *Comput. Mater. Sci.* **6**, 15

- (1996).
- [15] G. Kresse, D. Joubert, Phys. Rev. B **59**, 1758 (1999).
- [16] P. E. Blochl, Phys. Rev. B **50**, 17953 (1994).
- [17] H. Wende, D. Arvanitis, M. Tischer, R. Chauvistre, H. Henneken, F. May, K. Baberschke, Phys. Rev. B **54**, 5920 (1996).
- [18] F. M. Leibsle, Surf. Sci. **514**, 33 (2002).